Spectroscopy®
Solutions for Materials Analysis
September 2019 Volume 34 Number s9 www.spectroscopyonline.com

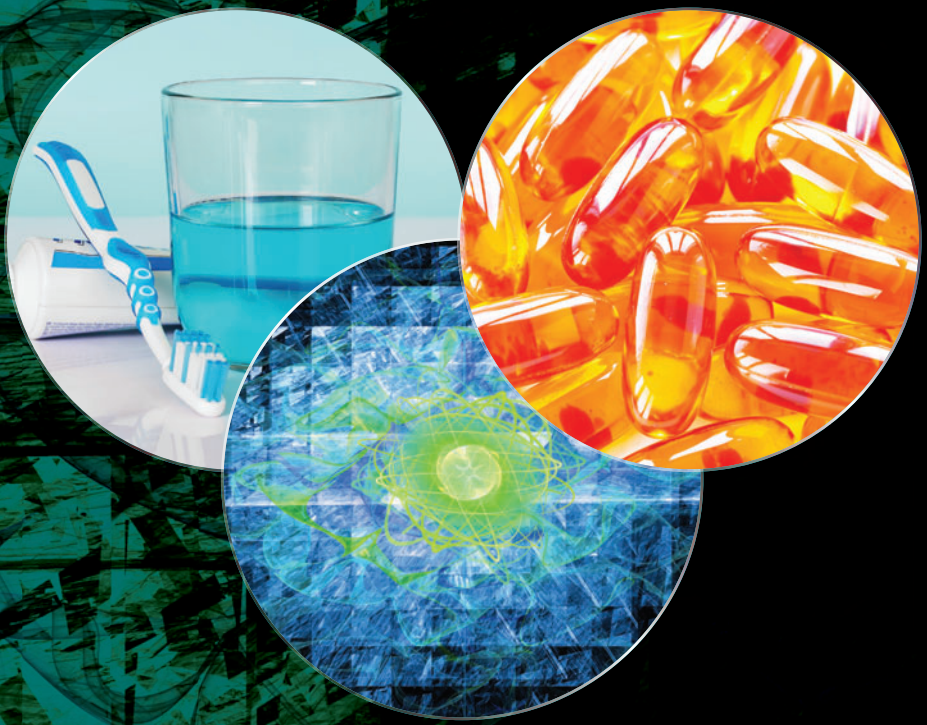

APPLICATIONS OF ICP-OES & ICP-MS

for Today's Spectroscopists

SHIMADZU
Excellence in Science

Accelerating
Reliable Performance

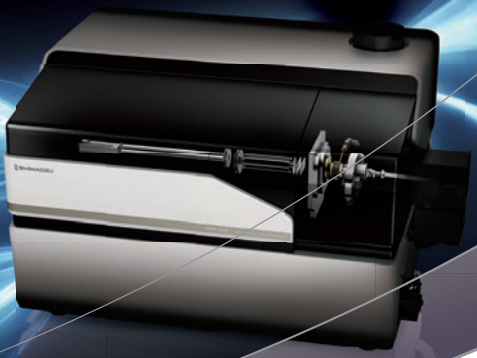

ICPMS-2030

Inductively Coupled Plasma Mass Spectrometer

Powered by its vast LC-MS/MS and GC-MS/MS experience, Shimadzu has released the **ICPMS-2030**, offering an exceptional combination of ease of use, high sensitivity, and low running costs. Simplify your ICP-MS analysis, and obtain reliable trace-level results with confidence. Choose the ICPMS-2030.

Key benefits include:

- **Fast, easy method development and acquisition of reliable results**
- **High sensitivity with no polyatomic interferences**
- **Lowest operation costs of any ICP-MS on the market**

Learn more about Shimadzu's ICPMS-2030.
Call (800) 477-1227 or visit us online at
www.ssi.shimadzu.com/ICPMS

Order consumables and accessories on-line at http://store.shimadzu.com
Shimadzu Scientific Instruments Inc., 7102 Riverwood Dr., Columbia, MD 21046, USA

Elemental Analysis • Environmental • Food & Agriculture • Pharmaceutical

50% reduction in cycle time

2X the throughput

50% lower labor costs

Numbers Don't Lie

Improved workflow

Maximum throughput

No batching required

Lower operating costs

With over a thousand units installed globally, Milestone's Single Reaction Chamber (SRC) technology has revolutionized how industrial and research laboratories around the world prep samples for analysis.

Our ultraWAVE transcends traditional closed and open vessel digestion, offering faster digestions, maximum throughput and lower cost of ownership.

High-performance stainless steel construction allows for higher pressures and temperatures and any combination of acids to be used, while disposable vessels eliminate the need to assemble, disassemble or clean between processing. Just as important, dissimilar samples can be processed simultaneously, saving time and resources. The bottom line? The Milestone ultraWAVE is the superior solution to handle all your sample prep challenges.

See what the ultraWAVE can do for your lab.

Visit us at www.milestonesci.com/ultrawave to schedule an onsite demonstration.

powered by milestone connect

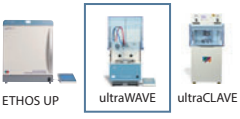

MILESTONE

Spectroscopy®

MANUSCRIPTS: To discuss possible article topics or obtain manuscript preparation guidelines, contact the editorial director at: (732) 346-3020, e-mail: LBush@mmhgroup.com. Publishers assume no responsibility for safety of artwork, photographs, or manuscripts. Every caution is taken to ensure accuracy, but publishers cannot accept responsibility for the information supplied herein or for any opinion expressed.

SUBSCRIPTIONS: For subscription information: *Spectroscopy,* P.O. Box 6196, Duluth, MN 55806-6196; (888) 527-7008, 7:00 a.m. to 6:00 p.m. CST. Outside the U.S., +1-218-740-6477. Delivery of *Spectroscopy* outside the U.S. is 3–14 days after printing. Single-copy price: U.S., $10.00 + $7.00 postage and handling ($17.00 total); Canada and Mexico, $12.00 + $7.00 postage and handling ($19.00 total); Other international, $15.00 + $7.00 postage and handling ($22.00 total).

CHANGE OF ADDRESS: Send change of address to *Spectroscopy,* P.O. Box 6196, Duluth, MN 55806-6196; provide old mailing label as well as new address; include ZIP or postal code. Allow 4–6 weeks for change. Alternately, go to the following URL for address changes or subscription renewal: http://ubmsubs.ubm.com/?pubid=SPEC

RETURN ALL UNDELIVERABLE CANADIAN ADDRESSES TO: IMEX Global Solutions, P.O. Box 25542, London, ON N6C 6B2, CANADA. PUBLICATIONS MAIL AGREEMENT No.40612608.

REPRINT SERVICES: Reprints of all articles in this issue and past issues are available (500 minimum). Licensing and Reuse of Content: Contact our official partner, Wright's Media, about available usages, license fees, and award seal artwork at Advanstar@wrightsmedia.com for more information. Please note that Wright's Media is the only authorized company that we've partnered with for MultiMedia Healthcare materials.

C.A.S.T. DATA AND LIST INFORMATION: Contact Melissa Stillwell, (218) 740-6831; e-mail: MStillwell@mmhgroup.com

INTERNATIONAL LICENSING: Alexa Rockenstein, e-mail: ARockenstein@mmhgroup.com

485F US Highway One South, Suite 210
Iselin, NJ 08830
(732) 596-0276
Fax: (732) 647-1235

Michael J. Tessalone
Group Vice President/MTessalone@mmhgroup.com

Stephanie Shaffer
Publisher/SShaffer@mmhgroup.com

Edward Fantuzzi
Associate Publisher/EFantuzzi@mmhgroup.com

Michael Kushner
Senior Director, Digital Media/MKushner@mmhgroup.com

Laura Bush
Editorial Director/LBush@mmhgroup.com

John Chasse
Managing Editor/JChasse@mmhgroup.com

Jerome Workman, Jr.
Senior Technical Editor/JWorkman@mmhgroup.com

Cindy Delonas
Associate Editor/CDelonas@mmhgroup.com

Allissa Marrapodi
Custom Content Writer/AMarrapodi@mmhgroup.com

Kristen Moore
Webcast Operations Manager/KMoore@mmhgroup.com

Vania Oliveira
Project Manager/VOliveira@mmhgroup.com

Sabina Advani
Digital Production Manager SAdvani@mmhgroup.com

Kaylynn Chiarello-Ebner
Managing Editor, Special Projects/ KEbner@mmhgroup.com

Dan Ward
Art Director/dward@hcl.com

Brianne Pangaro
Marketing Associate/BPangaro@mmhgroup.com

Melissa Stillwell
C.A.S.T. Data and List Information/MStillwell@mmhgroup.com

Alexa Rockenstein
Permissions/ARockenstein@mmhgroup.com

Jesse Singer
Production Manager/jsinger@hcl.com

Kelly Kemper
Audience Development Manager/KKemper@mmhgroup.com

Janet (Koehne) Roberts
Audience Support Analyst/JKoehne@mmhgroup.com

CORPORATE

Mike Hennessy, Sr.
Chairman and CEO/MHennessy@mjhassoc.com

Jack Lepping
Vice Chairman/JLepping@mjhassoc.com

Mike Hennessy, Jr.
President/MJHennessy@mjhassoc.com

George Glatcz
Chief Operations Officer/GGlatcz@mjhassoc.com

Neil Glasser, CPA/CFE
Chief Financial Officer/NGlasser@mdmag.com

Dave Esola
VP of Sales, Pharm Science/DEsola@mmhgroup.com

Engineered for Excellence

PlasmaQuant

PlasmaQuant MS I PlasmaQuant PQ 9000
Leading in ICP-MS and ICP-OES technology.

For more information, contact us:

info@us.analytik-jena.com
www.analytik-jena.com

analytikjena
An Endress+Hauser Company

Spectroscopy®

APPLICATIONS OF ICP-OES & ICP-MS FOR TODAY'S SPECTROSCOPISTS

SEPTEMBER 2019 VOLUME 34 NUMBER S9

Articles

Cover image courtesy of lisa_16/Adobe Stock; Maryia/Adobe Stock; LanaPo/Adobe Stock.

Osmium presents wicked problems because it can be dangerous and even deadly. It has a volatile personality, can change shapes, and even disappear and reappear during testing. It's easy to understand how even an experienced chemist can feel cowardly when working with Osmium.

For more information download our free white paper at **inorganicventures.com/osmium**.

REGISTERED ISO 9001 QSR-1034 BY QSR

ACCREDITED ISO 17025 0883.01 BY A2LA

ACCREDITED ISO 17034 0883.02 BY A2LA

INORGANIC™ VENTURES

inorganicventures.com

300 TECHNOLOGY DR. | CHRISTIANSBURG, VA 24073 USA | 800.669.6799

Arsenic Speciation in Krill and Other Marine Oils by Liquid Chromatography–Inductively Coupled Plasma-Mass Spectrometry

The content of total and inorganic arsenic was determined in krill oil, and the newly developed speciation method was carried out through a single laboratory validation. Krill oil samples were prepared by microwave digestion with the use of diluted nitric acid and hydrogen peroxide. Chromatographic separation of five arsenic species—arsenobetaine (AsB), dimethylarsinic acid (DMA), arsenite (AsIII), monomethylarsonic acid (MMA), and arsenate (AsV)—was achieved by high performance liquid chromatography (HPLC) using an anion exchange column and strongly basic carbonate eluent. Detection of the arsenic species was performed by inductively coupled plasma–mass spectrometry (ICP-MS). Signal drift was corrected by post column addition of an internal standard. Method performance was evaluated using percent mass balance of speciated arsenic versus total arsenic, and recovery of a fortified analytical portion (FAP). The average percent mass balance from replicate preparations of krill oil samples was 95%, and the recovery of FAP of all five species met the acceptance criteria of 95–105%. This procedure should prove useful when quantitating inorganic arsenic species in marine oils.

Katarzyna Banaszewski, Anna Plocicka-Okladlo, and Aaron Secrist

Krill (*Euphausia superba*) is a small crustacean commonly found in ocean waters around the world. It mainly serves as a food source for other aquatic creatures such as fish, penguins, and whales (1). In recent years, krill has gained more popularity in the natural product industry, and the krill oil became a promising dietary supplement, due to its high content of eicosapentaenoic

Savillex

fully automated high purity
Acid Production

DST-4000
Acid Purification System

High Purity, High Throughput
- ☐ Convert trace metal grade acid into high purity acid
- ☐ Purifies up to 4 L of HNO_3, HCl or HF per run
- ☐ Produces 1 L of 10 ppt grade acid in 12 hours

Simple Operation with Cost Savings
- ☐ Add acid, hit start and walk away
- ☐ Pays for itself in months, or even weeks

Operates Unattended
- ☐ Safe to operate unattended and overnight
- ☐ Acid level sensor switches power off when the run is completed

Learn More at
www.savillex.com

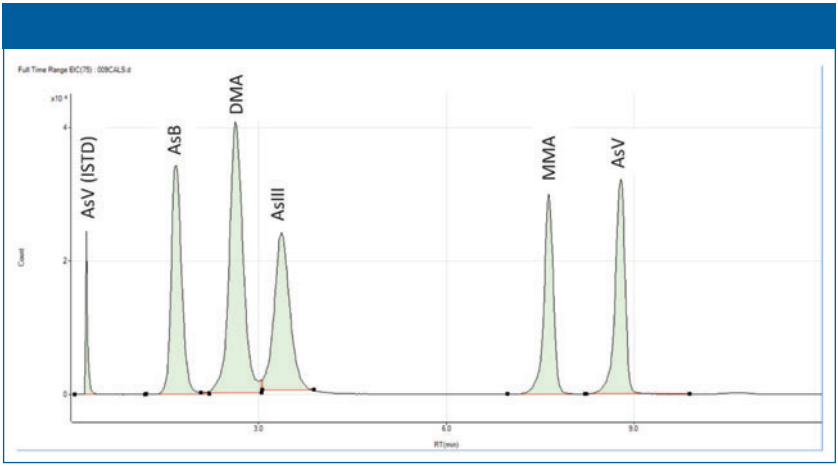

Figure 1: Chromatographic separation of five arsenic species in a standard solution.

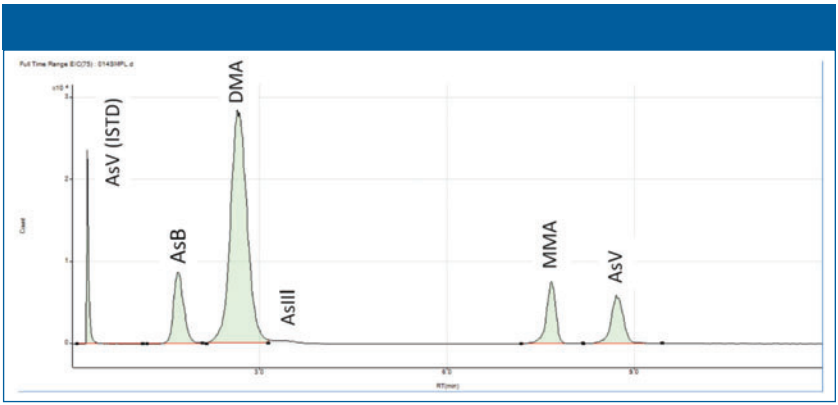

Figure 2: Chromatographic separation of detected arsenic species in krill oil.

acid (EPA), docosahexaenoic acid (DHA), and other health promoting compounds, such as astaxanthin (2). Although similar to fish oil, the omega-3 fatty acids in krill oil are structurally different. The omega-3 fatty acids in fish oil are triglyceride bound, whereas in krill oil they are in the form of phospholipids, which can impact the way they are being absorbed by the body. (3) Although supported by limited research, the potential krill oil health benefits include improvement of heart health, reduction of inflammation and arthritic pain, decreased incidences of obesity, and cancer prevention, as well as treatment for diabetes (4–6).

Although krill oil is rich in health promoting biomolecules, marine organisms tend to accumulate elements such as arsenic from the water. Arsenic is a ubiquitous element present in the environment, and its toxicity depends not

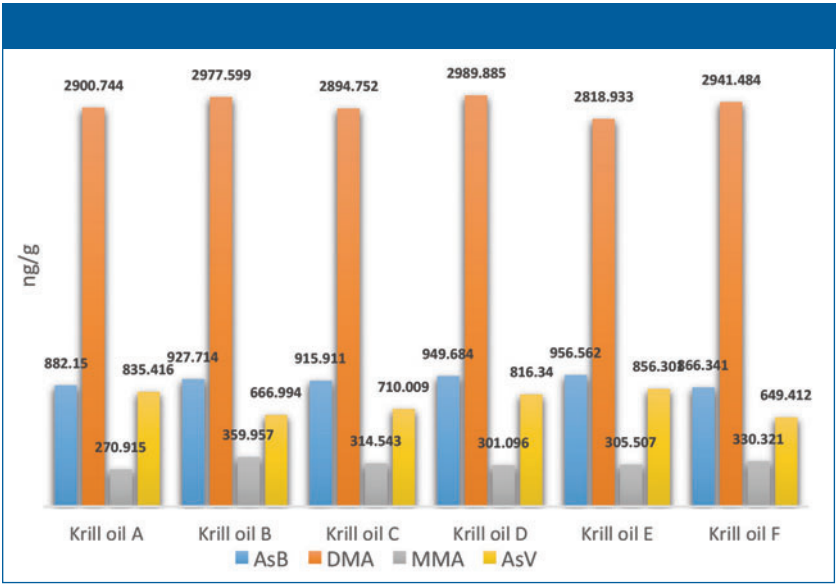

Figure 3: Reproducibility data of arsenic species determined in replicate preparations of krill oil.

only on total concentration, but more importantly on the chemical form of the element. In general, the inorganic arsenic species (AsIII and AsV) are considered to be the most toxic, whereas other organically bound species are considered to have lower or no toxicity in humans (7,8). There are many organic forms of arsenic, including methylarsonic acid (MMA) and dimethylarsinic acid (DMA), and the more complex arsenobetaine (AsB). Even though methylated arsenic species have been known to be less toxic than the inorganic species, to conduct a proper risk assessment all arsenic species present in the evaluated material should be identified. Although extensive literature has been published on the topic (9–11), arsenic speciation remains a challenging task, and requires thorough understanding of the species present in the analyzed matrix (12).

In recent years, the global demand for krill oil has been on the rise. The increasing popularity of this dietary ingredient has led to increased scrutiny by standard-setting bodies and government regulations around the world. In December 2017, the Food Chemicals Codex (FCC), a collection of internationally recognized standards for the purity and identity of food ingredients, released a monographed standard for krill oil. The aim of the monograph was to help promote quality krill oil identification and purity testing to strengthen the position of krill in the marketplace (13). Included in the requirements for krill oil are standards for EPA, DHA, phospholipids, and astaxanthin. The monograph also included a limit

Table I: Instrument operating conditions

ICP-MS Operating Parameters for Arsenic Speciation		ICP-MS Operating Parameters for Total Arsenic	HPLC Operating Parameters for Arsenic Speciation	
RF power	1550 W	1550 W	Column	Agilent anion exchange speciation column (4.6 mm x 150 mm)
Plasma gas flow	15 L/min	15 L/min		
Makeup gas flow	0.1 L/min	~0.2 L/min	Guard column	Hamilton PRP-X100
Nebulizer (carrier) gas flow	1.08 L/min	0.7–0.9 L/min	Mobile phase	A: 2.5 mM ammonium carbonate:0.2 mM EDTA:1% ethanol, pH 11.0 B: 100 mM ammonium carbonate:0.2 mM EDTA:1% ethanol, pH 11.0
Nebulyzer type	Glass concentric	Glass concentric	Mobile phase flow rate	1.0 mL/min
Peristaltic pump speed	0.3 rps	0.1 rps	Injection volume	100 µL
Spray chamber temp.	2 °C	2 °C	Column temperature	Ambient
Collision cell	HEHe @ 10.0 mL/min	He @ ~4.3 mL/min	Acquisition time	12 min
Data acquisition mode	Time-resolved, *m/z* 75 for $^{75}As^{+}$, and *m/z* 35 for $^{35}Cl^{+}$	Spectrum	Gradient	
Dwell time	0.8 s (*m/z* 75), 0.2 s (*m/z* 35)	0.51 s (*m/z* 75), 0.21 s (*m/z* 89)	Post Run	1 min
Replicates per ion	1	3	Switching valve time table	
Energy discriminator	7.0 volts	5.0 volts		

Time (min)	Mobile Phase A	Mobile Phase B
0	100%	0%
4	100%	0%
10	0%	100%
12	100%	0%

Time (min)	Column Position
0	1
0.2	2
0.7	1

for inorganic arsenic at NMT 0.1 mg/kg (14). The method defined in the monograph, which is not able to accurately differentiate between the chemical species of arsenic, cannot be compared with higher

Table II: Method detection and quantitation limits

Species	Retention Time (min)	Sensitivity (Peak Area/ ppb)	ASDL (ng/g)	ASQL (ng/g)	Method LOD (ng/g)	Method LOQ (ng/g)
AsB	1.69 ± 0.2	58237	0.08	0.5	16	100
DMA	2.63 ± 0.2	67785	0.08	0.5	16	100
AsIII	3.36 ± 0.2	49392	0.08	0.5	16	100
MMA	7.63 ± 0.3	59377	0.08	0.5	16	100
AsV	8.79 ± 0.4	101064	0.08	0.5	16	100

Table III: Summary of the precision data from the analysis of krill oil samples

Sample	AsB (ng/g)	DMA (ng/g)	AsIII (ng/g)	MMA (ng/g)	AsV (ng/g)	iAs (AsIII+AsV) (ng/g)	Total As	% Mass Balance
Krill Oil 1	927.7	2977.6	0	359.9	667.0	667.0	5145.0	96
Krill Oil 2	915.9	2894.8	0	314.5	710.0	710.0	5145.0	94
Krill Oil 3	866.3	2941.5	0	330.3	649.4	649.4	5145.0	94
Average	903.3	2938.0	0	334.9	675.5	675.5	5145	94.7
Stdev	32.6	41.5	NA	23.1	31.2	31.2	NA	NA
%RSD	3.6	1.4	NA	6.9	4.6	4.6	NA	NA

sensitivity and specificity speciation methods, such as HPLC–ICP-MS. Additionally, the complexity of the krill oil matrix requires suitable sample preparation able to liberate arsenic species, and allow for precise quantitation of inorganic arsenic. The aim of this study was to develop and validate a method for arsenic speciation and determination of inorganic arsenic in krill oil samples, and thus contribute to a more accurate risk assessment analysis regarding consumption of krill oil supplements.

Experimental

Samples

Samples of krill oil dietary supplements were purchased and found to be representative of the various krill oil suppliers present in the marketplace today.

Reagents

All reagents and solutions were prepared using ultrapure water purchased from EMD Millipore. Trace metal grade hydrochloric acid (HCl), nitric acid (HNO_3) and hydrogen peroxide (H_2O_2, 30%) were sourced from VWR Chemicals BDH. Ammonium carbonate ($CH_8N_2O_3$) was sourced from Alfa Aesar. Sodium hydroxide (50% in water), 200 proof ethanol, ethylenediaminetetraacetic acid disodium salt dehydrate (EDTA), and Triton X-100 were purchased from MilliporeSigma. Ultrahigh purity argon and helium were supplied by Airgas.

Determination of Total Arsenic by ICP-MS

The content of total arsenic in the krill oil was determined by ICP-MS. Briefly, samples of approximately 250 mg of homogenized krill oil were digested with 5 mL of HNO_3 and 0.5 mL of HCl in PTFE high pressure vessels using a microwave (Mars 6, CEM Corporation). After completion of the cycle, samples were cooled to room temperature, transferred into DigiTubes (SCP Science), and diluted to 50 mL with ultrapure water. Following additional 5x dilution with 2% HNO_3:0.5%HCl:0.01% Triton X-100, the total arsenic content in krill oil was determined using an Agilent 7700 ICP-MS instrument (Agilent Technologies). The instrument conditions are outlined in Table I. For total arsenic determination, a multielemental standard was used (SPEX Certiprep), and prepared in 2% HNO_3:0.5%HCl:0.01% Triton X-100 solution at concentrations ranging from 0 to 200 ng/g.

Determination of Inorganic Arsenic by HPLC-ICP-MS

For the determination of inorganic arsenic, approximately 250 mg of sample was weighed directly into a PTFE digestion vessel. Using a calibrated volumetric spigot, 5 mL of 0.28M HNO_3 was added to each sample, followed by 2.5 mL of hydrogen peroxide. Samples were digested using a progressive microwave program (Mars 6, CEM Corporation). The progressive power ramp from 290–1800 W was executed over 25 min, after which the samples were held for additional 25 min while heated at 210 ºC. The use of microwave and hydrogen peroxide in preparation of krill oil sample resulted in a cleaner digestate and more efficient extraction of arsenic from the matrix. Additionally, the quantitative oxidation of AsIII to AsV allowed the determination of total inorganic arsenic as a sum of AsIII and AsV. It has been previously verified that no conversion of organic species to inorganic arsenic occurs (15). Prior to analysis, the samples were transferred into a single use calibrated polypropylene DigiTubes (SCP Science), and diluted to 50 mL with 2.5 mM ammonium carbonate:0.2 mM EDTA:1% ethanol pH 11.0. Samples were filtered through PTFE syringe filters into polypropylene HPLC vials, capped, and submitted for HPLC-ICP-MS analysis.

Five standards were used for the speciation analysis: arsenite (AsIII) and arsenate (AsV) (1000 mg/L, Spex Certiprep), dimethylarsinic acid (DMA) (Alfa Aesar), monomethylarsonic acid (MMA) (ChemService, Inc.), and arsenobetaine (AsB) (Honeywell Fluka Chemicals) (Figure 1).

All stock solutions were prepared at 1000 µg/g, and their concentrations were based on elemental arsenic, rather than the molecular weight of the arseno compounds. All arsenic stock standards, except for As III and As V, which are traceable to NIST SRM, needed to be analyzed for total arsenic content to confirm the stock concentration. An intermediate solution was prepared at 200 ng/g, and used in preparation of working standards at concentrations ranging from 0.25–20 ng/g. Working arsenic standards were prepared in a solution of 2.5 mM ammonium carbonate:0.2 mM EDTA:1% ethanol pH 11.0. The analysis was performed using an

Agilent 1260 HPLC system (Agilent Technologies), consisting of a quaternary pump, autosampler, and a column compartment equipped with a six port switching valve. The chromatographic separation was achieved on an Agilent anion exchange speciation column (Agilent Technologies) (Figure 2).

An isocratic pump (Agilent Technologies) was used as an auxiliary pump for the introduction of an internal standard during the analysis. The internal standard (50 ng/g AsV in mobile phase A) was delivered to the switching valve using the isocratic pump post column through programmed column switching, using a 50 µL injection loop, which allows for signal drift monitoring and peak response correction. The speciated arsenic was determined with the use of Agilent 7700 ICP-MS (Agilent Technologies). The ICP-MS and HPLC conditions are shown in Table I.

Results and Discussion

Method Validation and Quality Control

The method was carried out through a single laboratory validation according to the ICH Analytical Method Validation Guidelines (16), following criteria for arsenic speciation described in Elemental Analysis Manual (EAM) 4.11 (17). Evaluated parameters included linearity, repeatability, intermediate precision, specificity, system suitability, limit of detection (LOD), and limit of quantitation (LOQ). In addition, the accuracy of a fortified analytical portion (FAP) was determined. As a part of quality control procedures, the percent mass balance was calculated between the sum of all arsenic species detected and the total arsenic determined in each sample.

An analytical solution detection limit (ASDL) and analytical solution quantitation limit (ASQL) was established for each analyzed arsenic species following the FDA's EAM, section 3.2 (18), and were based on standard deviation of replicate analyses of a low level mixed standard. The method limit of detection (LOD) and limit of quantitation (LOQ) were calculated using the ASDL and ASQL multiplied by the dilution factor. A summary of the method's detection and quantitation limits are summarized in Table II.

Calibration curves consisting of five points were established for all analyzed arsenic species, and were linear over the entire concentration range with $R^2 > 0.999$. Precision of replicate preparations of the krill oil sample ($n = 3$) was performed. The RSD limit for detected arsenic species in replicate preparations was set at <10%. The results from replicate preparations of the krill oil sample are summarized in Table III.

Intermediate precision data was obtained to demonstrate the method's performance over time. The RSD limit of all replicates ($n = 6$) was set at <15%, and met the criteria. Reproducibility data of arsenic species determined in replicate preparations of krill oil is shown in Figure 3.

The fortification (spike) recovery and precision was established for each of the arsenic species determined in the krill oil ($n = 3$). The sample was spiked with a mixed standard at 50% of the concentration determined for each arsenic species. The determination of FAP recoveries was performed through

standard addition, and the mean recoveries of spiked arsenic was within 94–105% for AsB, DMA, and MMA. Inorganic arsenic was determined as a sum of AsIII and AsV, and the recovery for total iAs was within 98–102%.

Mass balance was calculated between the sum of all arsenic species detected and the total arsenic determined in the krill oil sample. The percent mass balance was determined for each sample analyzed, and serves as a quality control measure to ensure that most of the arsenic is accounted for in the speciation analysis.

Due to lack of a certified reference material (CRM) for arsenic speciation in matrix similar to krill oil, trueness of the method performance could not be verified.

A large body of published literature reports arsenobetaine as the predominant organic arsenic form present in marine organisms (19–21); nonetheless, the most abundant arsenic species identified in krill oil samples appeared to be DMA. It was observed previously that the microwave digestion of samples in the presence of H_2O_2 oxidizes AsIII to the more stable AsV; however, a conversion of AsB to DMA has not been reported. To determine the native arsenic species present in krill oil, an alternate sample preparation was adapted to preserve the arsenic species.

Krill oil samples were prepared as described in EAM 4.11, and digested without the use of hydrogen peroxide in a heating block. Although the recovery of arsenic from the krill oil sample following another preparation was poor, the chromatographic separation of arsenic species confirmed the predominance of AsB. The mechanism of conversion of AsB to DMA under oxidative conditions is not clear; nevertheless, arsenobetaine degradation by microorganisms has been previously described by Hanoka and associates (1989) (22). Although the AsB to DMA conversion does not affect the iAs result or the determination of percent mass balance, it is worth mentioning that it changes the expected arsenic profile in material of marine origin.

Conclusion

An arsenic speciation method was developed and validated to provide a more accurate procedure for the determination of arsenic species in marine oils. The results obtained from this study demonstrated the method's applicability for determination of arsenic species in krill oil; however, it should be noted that the level of iAs detected in the analyzed krill oil exceeded the limit set by the FCC. The specificity of our method allows for more accurate iAs determination in such matrices compared to other published methods, and highlights the importance of using methods fit for purpose when establishing regulatory limits.

References

(1) J.M. Kwantes and O. Grundmann, *J. Diet. Suppl.* **12**(1), 23–35 (2015). doi: 10.3109/19390211.2014.902000

(2) J.C. Tou, J. Jaczynski, and Y.C. Chen, *Nutr. Rev.,* **65**(2), 63–77 (2007). doi. org/10.1111/j.1753-4887.2007.tb00283.x

(3) S. Ulven and K.B. Holven, *Vasc. Health Risk Manag.* **11**, 511–524 (2015). doi:10.2147/VHRM.S85165

(4) K. Yurko-Maur, J. Kralovec, E. Bailey-Hall, V. Smeberg, J. G. Star, and N. Salem, *Lipids Health Dis.* **14**, 99 (2015).

(5) N.F. Vigerust, B. Bjørndal, P. Bohov, and T. Brattelid, *TNF-α. Eur J Nutr* **52**, 1315 (2013).

(6) L. Deutsch, *J. Am. Coll. Nutr.* **26**(1), 39–48 (2007). doi:10.1080/07315724.2007.10719584

(7) K. Cheyns, H. Demaegdt, N. Waegeneers, A. Ruttens, "Arsenic Speciation Analysis Elucidates the Risk Assesment of Food Supplements with Ingredients of Marine Origin." 9th Nordic Conference on Plasma Spectrochemistry, Sciensano (2017)

(8) V. Sele, J.J. Sloth, A.K. Lundebye, E.H. Larsen, M.H.G. Berntssen, and H. Amlund, *Food Chem.* **133**, 618–630 (2012).

(9) J.J. Sloth, Abstract for the presentation at the EU-RL-ISS Workshop, October 7-8, 2013.

(10) A.A. Ammann, *Am. J. Anal. Chem.* **2**, 27–45 (2011).

(11) Z. Gong, X. Lu, M. Ma, C. Watt, and X.C. Le, *Talanta* **58**, 77–96 (2002).

(12) National Research Council (US) Subcommittee on Arsenic in Drinking Water. Arsenic in Drinking Water (National Academies Press, Washington, D.C., 1999), pp. 27–82.

(13) S. Daniels, *Supplier,* (2013) https://www.nutraingredients-usa.com/Article/2013/12/11/USP-monograph-strengthens-krill-s-position-in-the-marketplace-Suppliers

(14) 2018 USPC-Krill Oil-FCC Forum, December 2017

(15) E. H. Larsen, I. Rokkjaer, and T. Christensen, in *The Determination of Chemical Elements in Food: Applications for Atomic and Mass Spectrometry,* S. Caroli, Ed. (John Wiley & Sons, Hoboken, New Jersey, 2007), pp. 297–332.

(16) *International Conference on Harmonisation of Technical Requirements for Registration of Pharmaceuticals for Human Use, ICH Harmonised Tripartite Guideline, Validation of Analytical Procedures: Text and Methodology Q2 (R1),* Incorporated in November 2005.

(17) K. M. Kubachka, N. V. Shockey, T. A. Hanley, S. D. Conklin, and D. T. Heitkemper, *Arsenic Speciation in Rice and Rice Products Using High Performance Liquid Chromatography- Inductively Coupled Plasma-Mass Spectrometric Determination: FDA U.S. Food and Drug Administration Elemental Analysis Manual for Food and Related Products* (Food and Drug Administration, Silver Spring, Maryland, 2012)

(18) W. C. Cunningham, W. R. Mindak, S. G. Capar, *Elemental Analysis Manual* (Section 3.2 Terminology) (Food and Drug Administration, Silver Spring, Maryland, 2014)

(19) R. V. Hedegaard and J. J. Sloth, *Biothechnol. Agron. Soc. Environ.* **15(**S1), 45–51 (2011)

(20) R.V. Hedegaard, I. Rokkjaer, and J.J. Sloth, *Anal. Bioanal. Chem.* **405**(13), 4429–4435 (2013)

(21) P. Piras, R. Orletti, G. Chessa, C. Carloni, F. Griffoni, P. Palombo, and F. Velieri, *Ital. J. Food Saf.* **4(**1), 4577 (2015)

(22) K. Hanoka, K. Kazuhiko Ueno, S. Tagawa, and T. Kaise, *Comp. Biochem.* **94**(2), 379–382 (1989).

Katarzyna Banaszewski, Anna Plocicka-Okladlo, and Aaron Secrist are with NOW Foods, in Bloomingdale, Illinois. Direct correspondence to: k.banaszewski@nowfoods.com

Niagara CM Rapid

Saves Time & Money

The Niagara CM Rapid Rinse is the simplest, lowest-cost method of improving throughput on an existing ICP-OES or ICP-MS system. Increased throughput is achieved by rinsing the nebulizer and spray chamber the instant the sample measurement is completed and continuing to rinse until the next sample has reached the nebulizer.

- Faster sample turn around (~ 30%)
- Reduced operating costs
- Inert sample path, minimum carryover
- Easily interfaces to most ICP and autosampler models
- Faster washout
- Ability to handle complex samples

GLASS EXPANSION
Quality By Design

Rinse

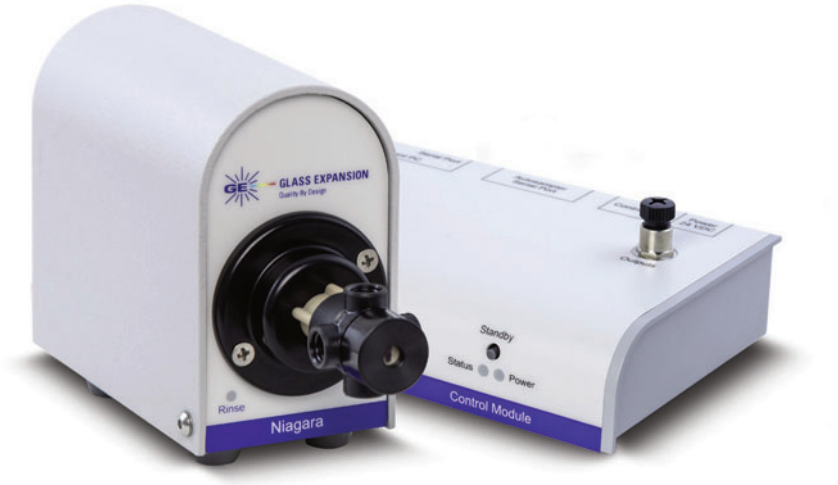

Comparison of ICP lab with and without the Niagara Rapid Rinse		
	Standard ICP	**With Niagara-CM**
Uptake Delay (sec	30	30
Stabilization (sec)	10	10
Total Read (sec)	60	60
Rinse (sec)	30	0
Total (sec)	130	100
Sample per Hour	27	36

31 Jonathan Bourne Drive, Unit 7 Pocasset, MA 02559
Toll Free (US): 800 208 0097
Email: geusa@geicp.com

Method Development with ICP-MS/MS: Tools and Techniques to Ensure Accurate Results in Reaction Mode

Since the launch of the first commercial triple-quadrupole ICP-MS (ICP-MS/MS) instrument in 2012, the technique has become well established in both research and academic institutes, as well as in industrial and commercial laboratories. Users in routine applications wish to benefit from the improved interference removal performance of ICP-MS/MS, without facing the more complex method development inherent in the use of ion-molecule reaction chemistry. In this article, we follow method setup and optimization steps to illustrate how an ICP-MS/MS method can be defined and tested to ensure consistent performance.

Ed McCurdy, Glenn Woods, and Naoki Sugiyama

Single-quadrupole inductively coupled plasma–mass spectrometry (ICP-MS) provides performance that meets the needs of most inorganic (metals) analysis laboratories, and exceeds the method requirements for many. The technique offers a unique combination of fast multielement analysis, good elemental coverage, very low detection limits, and the ability to measure major and trace elements in a single acquisition. The development of collision–reaction cells (CRCs) operating in helium collision mode addressed many of the polyatomic interferences that previously hampered accurate analysis of several critical trace elements (1). However, helium mode cannot resolve interferences such as isobaric and doubly charged overlaps. Also, some combinations of analyte and interference require more effective attenuation of the overlap than can be achieved using collision mode and kinetic energy discrimination (KED). For these cases, ion-molecule reaction chemistry using a reactive cell gas may offer a better solution.

Reactive cell gas methods have been investigated since CRCs were first developed for single-quadrupole ICP-MS in the late 1990s (2). Early work presented the benefits of reaction chemistry for histori-

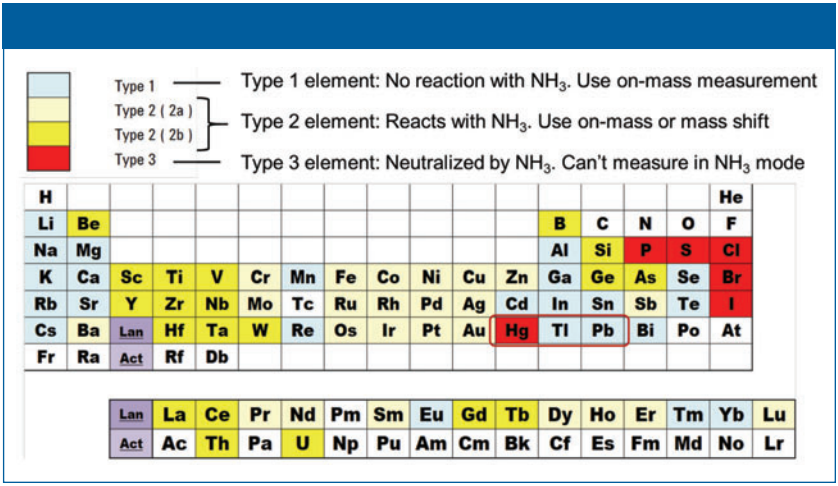

Figure 1: Reaction pathways and rates for all analyte ions with NH_3 cell gas derived from reference 10. Hg and Pb are highlighted, showing how reaction data can be used to identify the potential to resolve the isobaric overlap from ^{204}Hg on ^{204}Pb.

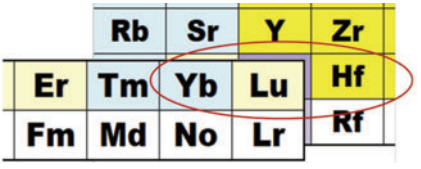

Figure 2: Reaction data indicates NH_3 may be a suitable cell gas to resolve Yb and Lu overlaps on Hf (refer to Figure 1 for key to color-coding of NH_3-reactions for each element).

cally problematic analytes that suffer intense spectral overlap (such as selenium, arsenic, iron, calcium, and so on). However, these early applications were often based on the theoretical efficiency of the reaction chemistry to resolve one specific interference, and were illustrated using simple, consistent samples or synthetic solutions. Often, when these methods were applied to more complex and variable natural samples, it became apparent that the reaction processes could be adversely affected by other components in the sample (3,4). An unexpected matrix element or co-existing analyte could react with the cell gas, forming unwanted overlaps on the analyte ion (or product ion). Consequently, a reaction gas method developed for one sample matrix or interference might give erroneous results for a different sample type or combination of analytes.

The development of triple quadrupole ICP-MS (ICP-MS/MS) in

2012 offered a solution to the inaccurate results observed when using reactive cell gases on single quadrupole instruments (5). ICP-MS/MS has an additional quadrupole mass filter (Q1) before the CRC, in a tandem mass spectrometer (MS/MS) configuration. When Q1 is operated as a true mass filter (1 u mass window), it controls the ions passed to the cell, rejecting all nontarget masses. This means the reaction processes and product ions formed are predictable and consistent, and are unaffected by other analytes or matrix elements in the sample (6).

In addition to improving data quality, the control of reaction chemistry provided by ICP-MS/MS means that method settings can be applied consistently, even for variable samples. This makes reaction mode method setup easier than on a single quadrupole instrument or a configuration with a bandpass filter (mass window >1 u) before the cell. In this article, we illustrate the information and tools available for ICP-MS/MS to support development and performance testing of a new reaction mode method.

Reference Methods for Reactive Cell Gas Operation with ICP-MS/MS

Since the first commercial ICP-MS/MS instrument was released in 2012, many applications have been developed, optimized, and published. In addition to manufacturers' application notes (7), many hundreds of peer-reviewed journal articles detail method settings for both typical and unusual applications.

The ICP-MS/MS instrument's built-in methods can predefine the typical cell gas mode, analyte and product ion masses, and integration times for common analytes. Where an analyte does not have an established setting predefined in a preset method, the user can easily set up one or more mass pairs for the chosen reaction gas. The choice of reaction gas used to resolve a specific interference can be informed by the literature. Theoretical ion-molecule reaction thermodynamics show which reactions are favored (8,9), while ICP-MS/MS manufacturer's publications show experimental results for various product ion formation rates. Hydrogen (H_2) oxygen (O_2) and ammonia (NH_3) are among the most widely-used reaction gases. For each gas, several common reaction transitions are defined in the literature, and have been confirmed experimentally (10).

With oxygen cell gas, for example, analytes may be measured on mass (Q2 is set to the same mass as Q1) or mass shifted as the oxide ion (Q2 is set to Q1 + 16 u) or dioxide ion (Q2 is set to Q1 + 32 u). These mass shift transitions, together with equivalent transitions for other reaction gases, are available as preset values in the method setup software, allowing easy selection of the preferred mass shift. Multiple mass shifts can be selected if the user wants to compare results for several product ions or cell gases, and custom mass shifts can be defined, if appropriate.

Table I: Typical reactions of elemental cations with NH_3 cell gas

Chemical Reactions of Cations (M^+) with NH_3 Cell Gas	
Charge transfer*	$M^+ + NH_3 \rightarrow M + NH_3^+$
Recombination	$M^+ + NH_3 \rightarrow MNH^+ + H_2$ or $M^+ + NH_3 \rightarrow MNH_2^+ + H$
Clustering	$M^+ + NH_3 \rightarrow MNH_3^+$, $M(NH_3)_2^+ \ldots M(NH_3)_n^+$

*Charge transfer is useful for removing an isobaric overlap on a target analyte ion. It is not used for analyte measurement because the elemental ion is neutralized

In the case of NH_3 cell gas, reactions are usually fast and are often sequential, so multiple cluster ions can form from both the analyte ions and any other ions present in the cell. Typical reactions and product ions formed with NH_3 cell gas are shown in Table I. MS/MS mode controls the precursor ions that can enter the cell and react, so product ions can only form from ions at the mass of the target analyte ion. However, optimized methods must still be verified to confirm that the chosen reaction product ion is free from overlap by product ions from other sample components present at the same mass as the analyte precursor ion.

Product Ion Scanning

Product ion scanning, which is unique to MS/MS, is a useful method development tool for unfamiliar sample types and unusual combinations of analyte interferences. This mode enables users to check and verify the best product ion(s) to use by identifying product ions that are free from overlap in a given sample type or matrix. This is particularly useful for complex and variable sample matrices, and for the large number of product ions produced when a highly reactive cell gas such as NH_3 is used.

In a product ion scan, Q1 is set to the mass of the target analyte isotope, and Q2 is scanned across the mass range where useful product ions could appear. It is essential that Q1 is operated at 1 u resolution, so only ions at the target analyte isotope mass enter the cell. A product ion scan is acquired while aspirating a single-element standard of the target analyte, allowing product ions formed from the analyte isotope alone to be identified. A second product ion scan is then acquired while aspirating the unknown sample or synthetic matrix to identify product ions formed from other (nontarget) precursor ions at the target analyte mass. By comparing the spectra from the two scans, analyte product ions that are free from overlap by matrix product ions can easily be identified (11).

Experimental

Instrumentation and Reagents

An Agilent 8900 ICP-MS/MS instrument (model #100, Advanced Applications configuration) was used for all measurements. The instrument was fitted with the

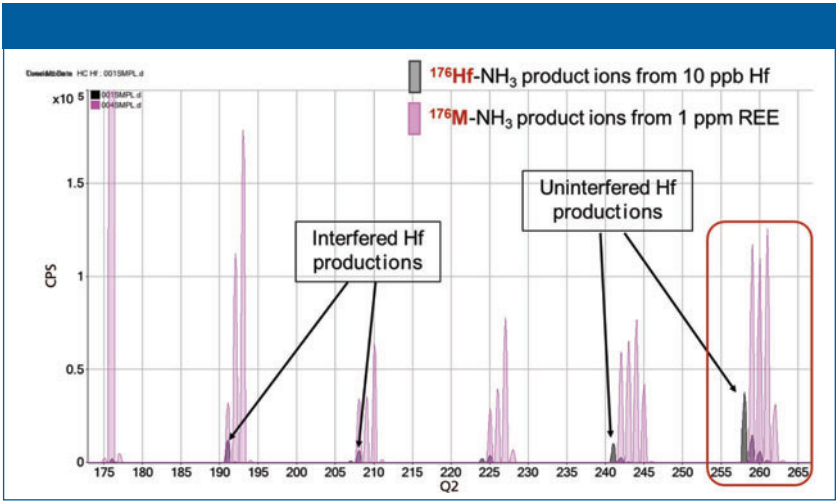

Figure 3: Overlaid spectra for NH_3 product ions formed from *m/z* 176 in Hf standard (gray) and REE mix (pink), showing overlapped and interference-free Hf-NH_3 product ions.

standard glass concentric nebulizer, quartz spray chamber, quartz torch with 2.5 mm injector, and standard nickel sampling and skimmer cones. Samples were introduced via a peristaltic pump with 1.02-mm i.d. pump tubing. Operating conditions are shown in Table II.

The hafnium standard was prepared from a single element stock solution, and the rare earth matrix was prepared from a mixed 14-element stock standard (Agilent Technologies). Ultrapure water was prepared in the laboratory using a Milli-Q Element system, and nitric and hydrochloric acids used for sample stabilization were Ultrapure NORMATOM grade (VWR Chemicals).

Hf and mixed rare earth elements (REE) standards were prepared at 10 ppb and 1 ppm, respectively, in a final diluent of 2% HNO_3 and 1% HCl. A spike solution of 10 ppb Hf in 1 ppm REE mix was also prepared.

Results and Discussion

Choosing Reaction Gas Modes to Resolve Known Interferences

Theoretical ion-molecule reaction rates can be used to identify potential approaches to resolve a given interference, based on differences in the reactions for the analyte and interfering ion. Figure 1 shows the reactions of all elemental ions with ammonia cell gas (10), displayed in a color-coded periodic table layout. To illustrate how this information can be used, the different reactions of Hg^+ and Pb^+ with NH_3 are highlighted in the table. Mercury (a Type 3 element) reacts with NH_3 cell gas via a charge-transfer reaction leading to the neutralization of the Hg^+ ion. In contrast, Pb (a Type 1 element) does not react with NH_3, so it can be measured on mass. The difference in reactions of Hg and Pb ions indicates that NH_3 could be a suitable

Table II: ICP-MS/MS operating conditions and acquisition parameters for ^{176}Hf product ion scanning with NH_3 cell gas

Parameter	Instrument Conditions	
Forward RF power (W)	1500	
Nebulizer gas flow (L/min)	0.7	
Makeup gas flow (L/min)	0.5	
Sampling depth (mm)	8	
Extraction lens 1 (V)	-2	
Extraction lens 2 (V)	-200	
Octopole bias (V)	-4	
KED (V)	-8	
Axial acceleration (V)	0.5	
Cell gas mode	NH_3	
Cell gas flow (mL/min) (MFC setting in brackets)	He: 1.0; NH_3: 2.0 (20%);	
Acquisition conditions		
Q1 Mode	MS/MS	Bandpass
Q1 mass range (*m/z*)	176	175 to 177
Q2 Mass range (*m/z*)	175 → 265	

cell gas to resolve the ^{204}Hg overlap on ^{204}Pb, allowing accurate analysis of ^{204}Pb on mass at *m/z* 204.

In the case of hafnium analysis in a rare earth element matrix, the reaction data presented in Figure 1 suggests that NH_3 cell gas might be able to resolve the Yb and Lu overlaps on Hf. The ^{178}Hf isotope is the preferred isotope for quantitative analysis, but ^{176}Hf is required for some applications such as Hf/Lu and Hf/Hf isotope geochronology. The ^{176}Hf isotope could be considered the worst case in terms of interferences in sample matrices that contain REEs. As well as direct isobaric interferences from ^{176}Yb and ^{176}Lu,^{176}Hf is also overlapped by oxide ions of ^{160}Gd and ^{160}Dy. Figure 2 shows that Hf (a Type 2b element) reacts with NH_3 cell gas, whereas Yb (a Type 1 element) does not. Hafnium will therefore form Hf-NH_3 product ions that cannot be overlapped by corresponding NH_3 product ions formed from Yb.

The same principle does not necessarily apply to resolving the ^{176}Lu isobaric overlap on ^{176}Hf. Lu is a Type 2a element, so it does react with NH_3, and may form product ions that can overlap the Hf-NH_3 product ions. Also, ion-molecule reaction data does not give specific information about the potential for a given cell gas to resolve polyatomic overlaps, such as the $^{160}Gd^{16}O$ and $^{160}Dy^{16}O$ interferences on ^{176}Hf. The solution to confirming the suitability of a given reaction gas to resolve

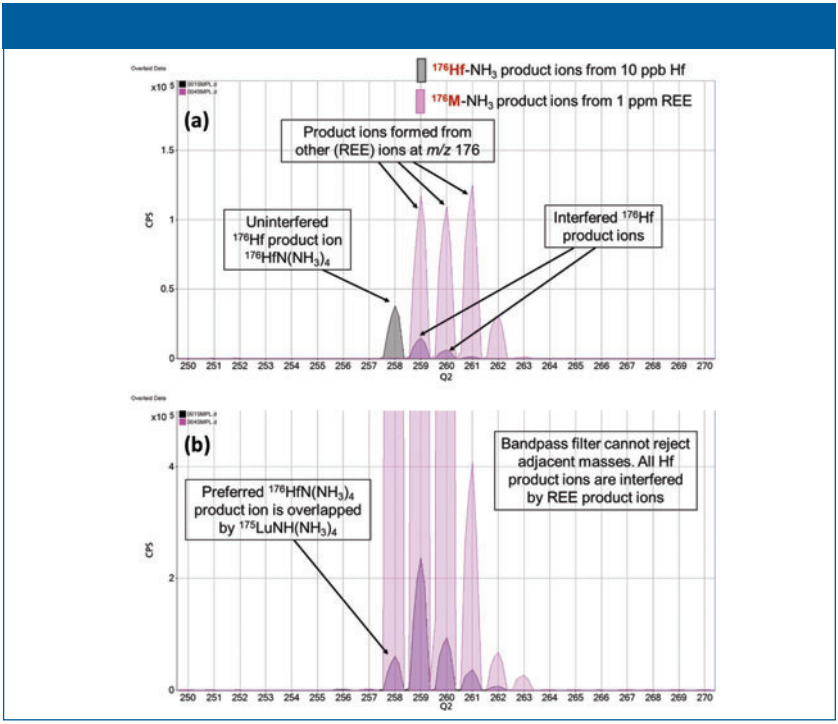

Figure 4: Detail showing NH_3 product ions in the mass range around the preferred ^{176}Hf product ion at *m/z* 258. In (a) MS-MS mode, $^{176}HfN(NH_3)_4$ is free from any REE product ion overlap. (b) In simulated 3 u bandpass mode, ^{175}Lu is not excluded from the cell, so $^{175}LuNH(NH_3)_4$ is formed, overlapping $^{176}HfN(NH_3)_4$ at *m/z* 258.

such interferences is to verify the performance experimentally by using a product ion scan.

Identifying Interference-free Hf-NH_3 Product Ions in REE Matrix Using Product Ion Scanning

For analytes, interferences, and sample types that are not defined in preset methods or available from reference publications, product ion scanning can identify the best product ion(s) for the application. Product ion spectra were acquired for a 10 ppb Hf standard and a 1 ppm 14-element REE mix. An overlay of the two product ion spectra covering the mass range from *m/z* 175 to 265 is shown in Figure 3. The spectrum comparison facilitates identification of product ions formed from *m/z* 176 precursor ions in the Hf standard but not the REE mix. The most intense interference-free ^{176}Hf product ion identified was $^{176}HfN(NH_3)_4^+$, which appears at *m/z* 258. This Hf product ion is free from any REE-based overlap—that is, no overlapping NH_3 product ions are formed from Lu and GdO/DyO precursor ions present at *m/z* 176.

In this example, the REE-based overlaps being investigated were known in advance, so a synthetic standard solution could be prepared, ensuring the creation of the interfering REE-NH_3 product ions. For complex sample matrices, which might give rise

to unknown product ions, the product ion scan can be performed for a real sample matrix. In this way, potential overlaps from all sample components can be checked and accounted for during method development.

Controlling Product Ion Formation with MS/MS vs. Single Quadrupole or Bandpass

Product ion scanning—and the MS/MS methods developed using it — rely on Q1 operating at unit mass resolution (1 u mass window). The necessity for this is illustrated in Figure 4, where normal Agilent 8900 MS/MS operation is compared to deliberately "detuned" operation where Q1 has been set to pass a 3 u mass range. This simulates ICP-MS operation with a bandpass filter rather than a unit mass filter before the cell.

The top spectrum in Figure 4 shows the mass range from *m/z* 250 to 270 extracted from the full mass product ion spectra in MS/MS mode shown in Figure 3. This includes the preferred, interference-free $^{176}HfN(NH_3)_4^+$ product ion at *m/z* 258. The lower spectrum shows the same mass range for the same product ion scans for the 10 ppb Hf and 1 ppm REE solutions, acquired with 3 u bandpass mode. With a bandpass filter before the cell, adjacent precursor ions are not rejected, so they enter the cell and react. In this example, with Q1 passing a 3 u range of masses around the set mass, ^{175}Lu can enter the cell when the precursor ion mass is set to *m/z* 176. ^{175}Lu reacts with NH_3 cell gas to form a product ion $^{175}LuNH(NH_3)_4^+$, which appears at *m/z* 258, overlapping the preferred $^{176}HfH(NH_3)_4^+$ product ion used for ^{176}Hf analysis.

The example of interferences on Hf product ions in a REE matrix illustrates a general limitation of incomplete rejection of adjacent masses before the cell when using highly reactive cell gases. Any nontarget ions that enter the cell may react to form overlapping product ions, giving errors on the target analyte product ion mass.

Conclusions

Triple-quadrupole ICP-MS is often perceived as being more complicated and difficult to setup than single-quadrupole ICP-MS. However, the main benefit of the MS/MS tandem mass spectrometer configuration is the superior control it offers with reactive cell gas methods for interference removal. For these reaction gas methods, the ability of MS/MS to select the specific mass that is passed to the cell provides much greater control of the reaction chemistry. Rejecting nontarget, off-mass elements and isotopes using Q1 means these ions cannot enter the cell and affect the reaction processes. As a result, reaction gas methods on ICP-MS/MS are more consistent, more reliable, less matrix dependent, and therefore easier to setup than on single quadrupole ICP-MS.

References

(1) E. McCurdy and G. Woods, *J. Anal. At. Spectrom.* **19**, 607–615 (2004).

(2) S.D. Tanner and V.I. Baranov, *J. Am. Soc. Mass Spectrom.* **10**, 1083–1094 (1999).

(3) L.J. Moens, F.F. Vanhaecke, D.R. Bandura, V.I. Baranov, and S.D. Tanner, *J. Anal. At. Spectrom.* **16**, 991–994 (2001).

Continued on page 34

Development of an Analytical Method to Determine Chromium, Iron, Nickel, and Zinc in Mouthwash by ICP-OES and Assessment of Possible Metal Migration from Stainless Steel

Mouthwash is a commonly used oral care product. Because of its composition, it is considered a complex matrix for elemental analysis. This work describes a simple analytical method, requiring no sample pretreatment, for determination of chromium, iron, nickel, and zinc in mouthwash by inductively coupled plasma–optical emission spectrometry (ICP-OES). To study the possible matrix effect on the calibration, a comparison was made between calibrations by matrix-matched and external standards. Excellent detection limits were obtained for chromium, iron, nickel, and zinc (16.0, 23.0, 5.0, and 7.0 µg/L, respectively). In all of the strategies that were used, the linear range of the calibration curve was 30.0 µg/L to 9.0 mg/L (a wide linear range) with a coefficient of determination (R^2) > 0.9900. The proposed method was employed both in the determination of zinc, present as an ingredient in certain mouthwashes, and in the evaluation of possible migration by iron, chromium, and nickel from the stainless steel.

P.M.F. Camargo Filho, J.F.S. Joca, and I. Gaubeur

The use of mouthwash for oral care is a common practice. Ease of use, coupled with their effectiveness in preventing and controlling common mouth diseases, generates great demand for these products (1).

Mouthwashes containing zinc salts (such as chloride, citrate, and lactate), mainly associated with other actives such as chlorhexidine and cetylpyridinium chloride, have been shown to be effective in combating halitosis (2–4). In addi-

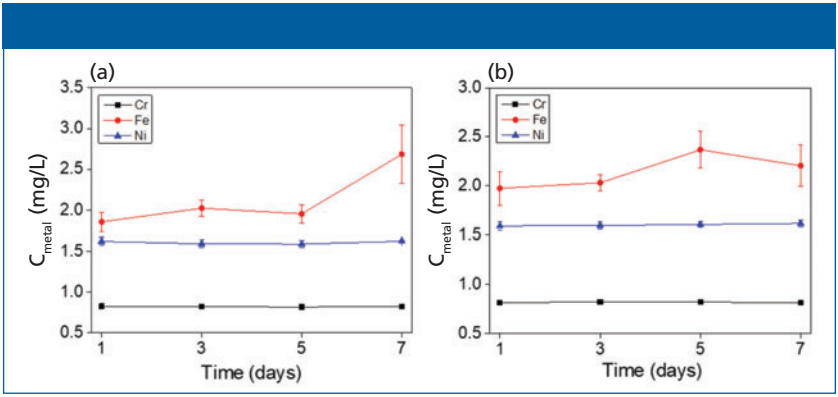

Figure 1: Fe, Cr, and Ni concentrations (C_{metal}) as a function of contact time in mouthwash samples containing (a) zinc salts, and (b) zinc-free.

Table I: Instrument and method parameters

Experimental Parameter	Value
RF generator power	1000 W
Plasma gas flow rate	15 L/min
Auxiliary gas flow rate	1.5 L/min
Nebulyzer type	Concentric glass
Spray chamber	Double pass cyclonic spray
Nebulizer gas flow	0.75 mL/min
Sample flow rate	0.5 mL/min
Sample uptake delay	10 s
Fast pump during the sample uptake	Yes
Pump speed	5 rpm
Stabilization time	5 s
Replicates	3
Read time	5 s
Analytical lines	Cr (II) – 267.716 nm Fe (II) – 238.204 nm Ni (II) – 231.604 nm Zn (I) – 213.857 nm

tion, zinc has low toxicity and does not stain teeth (5).

Metal migration to mouthwashes is reported in the literature (6,7), focusing on the corrosion studies of orthodontic appliances (also produced in stainless steel). Elemental analysis is usually performed by graphite furnace atomic absorption spectrometry (GF-AAS) (6,7) or inductively coupled plasma mass spectrometry (ICP-MS) (8). In spite of the use of inductively coupled plasma-optical emission spectrometry (ICP-OES) (9) having

Table II: Statistical comparison of the angular coefficients of the different calibration curves

Analyte	Calibration	A	Student's t-Value
Chromium	EC $MM_{0.4}$ MM_{20}	11930 ± 110 12120 ± 120 9619 ± 90	t_{calc} 1.94 26.7
Iron	EC $MM_{0.4}$ MM_{20}	11920 ± 110 11900 ± 290 9221 ± 81	t_{calc} 0.11 34.2
Nickel	EC $MM_{0.4}$ MM_{20}	1786 ± 25 1823 ± 20 1356 ± 15	t_{calc} 2.00 25.5
Zinc	EC $MM_{0.4}$ MM_{20}	6613 ± 93 6770 ± 140 6107 ± 50	t_{calc} 1.62 8.30

A: Angular Coefficient (slope)
EC: External Calibration (2.0% HNO_3)
$MM_{0.4}$: Matrix Matched Calibration in 0.4% mouthwash
MM_{20}: Matrix Matched Calibration in 20% mouthwash
t_{calc}: Student's t value compared to EC with 99% of confidence level

been demonstrated, there is a lack of studies that carefully evaluate the matrix effects of mouthwashes on the analytical signals in spectroscopic techniques.

Here, we propose a simple analytical procedure based on dilution or matrix-matched calibration, which allows the quantification of chromium, iron, nickel, and zinc in mouthwash without needing complex sample preparation or extraction. The procedure is aimed at quantification of zinc in these products as an ingredient and at chromium, iron, and nickel after migration test from the stainless steel.

Experimental

ICP-OES System

All measurements were performed using a Varian 710-ES ICP-OES instrument, in axial view. Instrumental and operating parameters are shown in Table I.

Calibration Standards

Calibration standards were prepared at concentrations from 30.0 µg/L to 9.0 mg/L by diluting 1000 mg/L stock standards (SpecSol). After matrix effect evaluation for zinc quantification in four commercial samples, the standards were diluted in 2.0% HNO_3 solution, produced with deionized water with resistivity ≥18.2 MΩ cm (obtained from a Millipore Milli-Q system), for dilution of 65% HNO_3 obtained from Sigma Aldrich. Quantification of chromium, iron, and nickel in metal migration studies was performed by "matrix-matched" calibration, and the standards were diluted in a solution containing 20% of a chromium-, iron-, nickel- and zinc-free mouthwash and 2.0% HNO_3, prepared as described above.

Calibration Strategies and Matrix Effect Evaluation

Calibration curves were constructed in three ways: 1) external calibra-

Table III: Recovery for chromium, iron, nickel, and zinc

Analyte	Recovery (%)
Chromium	102±2
Iron	102±1
Nickel	103±1
Zinc	103±1

Table IV: Zinc quantification in commercial samples

Sample	Zinc (mg/L)
1	671 ± 4
2	739 ± 19
3	863 ± 10
4	409 ± 10

tion (2.0% HNO_3 media); 2) matrix-matched calibration in 20% chromium-, iron-, nickel- and zinc-free mouthwash (standards contain mouthwash diluted fivefold); and 3) matrix-matched calibration in 0.4% rinse chromium-, iron-, nickel-, and zinc-free mouthwash (standards contain mouthwash diluted 250-fold). Angular coefficients of the calibration curves ($n = 3$ for each curve) were statistically compared by Student's *t*-test, at a 99% confidence level, to detect significant differences in their angular coefficients and the consequent matrix effect. The mouthwash used to prepare the standards was previously diluted fivefold in 2.0% HNO_3 solution, and the analytical signals obtained for the elements of interest were comparable to the analytical blank (2.0% HNO_3).

Studies on Metal Migration from Stainless Steel

Stainless steel 316L samples 1.0 mm thick and 5.0 mm wide were immersed in hexane for 5 min to remove oils and greases. Next, the samples were rinsed with water, then rinsed with absolute ethanol. Finally, samples were dried at room temperature.

To evaluate the possible migration of iron, chromium, and nickel from stainless steel to the mouthwash, approximately 0.350 g stainless steel segments were added to 24 polypropylene tubes (one segment per tube), which were divided into 2 groups of 12 tubes. To the first group was added 3.0 mL of a mouthwash containing zinc salts in its composition, and to the second group was added 3.0 mL of a similar mouthwash, but zinc-free.

Tubes with mouthwashes and stainless steel segments were stored at room temperature, and were manually shaken for 5 min every 12 h for a total of 7 days. After 1, 3, 5, and 7 days of contact with stainless steel, 1.50 mL aliquots ($n = 3$ for each contact time) were removed from the tubes, acidified with 0.50 mL of 2.0% HNO_3 and refrigerated for subsequent ICP-OES analysis.

Results and Discussion

Matrix Effect Evaluation

It is usual to perform acid digestion for elemental determinations by spectroscopic techniques in pharmaceutical and cosmetic samples (10,11). Mouthwash contains substances (such as surfactants, preservatives, and saline compounds) that change the sample's surface tension, viscosity, and, consequently, transport efficiency in the ICP-OES nebulization system (12), besides conferring high carbon levels in the matrix, which is undesirable in ICP-OES analysis. Methods that circumvent the difficulties of the matrix

effect without performing acid digestions are interesting for routine analysis and increase the analytical frequency.

Table II shows the angular coefficients obtained in the external calibration and matrix-matched calibrations containing 0.4% and 20% iron-, chromium-, and nickel-free mouthwash and the Student's *t*-value calculated for a 99% confidence level.

There are no significant differences between the angular coefficients of the EC and $MM_{0.4}$ curves; therefore, for the analysis of a mouthwash with a dilution of 250-fold, external calibration can be used because there is no significant matrix effect on the analytical signals of chromium, iron, nickel, and zinc. The comparison between EC and MM_{20} angular coefficients shows statistically significant differences, evidenced by the calculated Student's *t*-values, which are much higher than the critical value (4.604) for all analytes. Thus, for the analysis of a mouthwash with a dilution of fivefold, external calibration cannot be used because the matrix effects are significant. The lower angular coefficients of MM_{20} in relation to EC indicates that the mouthwash matrix, if present in high concentrations, promotes suppression of the analytical signals of chromium, iron, nickel, and zinc.

Recovery Test

To evaluate the accuracy of the proposed method, 1.0 mL of a stock solution containing 1000 mg/L of chromium, iron, nickel and zinc was diluted in a 20 mL solution of iron-, chromium-, nickel-, and zinc-free mouthwash. Then 40 µL of this solution was diluted in 10 mL of 2.0% HNO_3 solution. Next, the solution was analyzed ($n = 3$) using external calibration. Recoveries are shown in Table III.

Quantification of Metal Migration from Stainless Steel

The literature reports migration tests in which samples are immersed in different corrosive media, such as artificial saliva, mouthwash, and saline solutions (7,13,14). Usually, the evaluation of corrosion is verified by microscopy.

To quantify chromium, iron, and nickel, the MM_{20} calibration was adopted. 1.0 mL of each previously acidified sample was diluted in 5.0 mL of 2.0% HNO_3 solution and analyzed by ICP-OES. Figure 1 shows the variation in iron, chromium, and nickel concentrations (C_{metal}) as a function of contact time in mouthwashes containing (a) zinc salts and (b) zinc-free.

After the first day of contact, migration of chromium, iron, and nickel to the mouthwashes occurs. Chromium and nickel concentrations did not significantly change over the 7 days of testing for either evaluated formulation.

Iron concentration in mouthwash containing zinc salts shows an increase between the 5th and 7th days (Figure 1a), but the values do not differ significantly at a 99% confidence level according to the Student's *t*-test ($t_{calculated} = 2.216$ and $t_{critical} = 4.604$). Also verified was an increase in iron concentration in the zinc-free mouthwash on day 5 (Figure 1b), but there was no significant difference between concentrations on days 5 and 7 at a confidence level of 99% ($t_{calculated} = 1.040$ and $t_{critical} = 4.604$).

Limits of detection (LODs) for chromium, iron, and nickel were 16.0, 23.0 and 5.0 µg/L, respectively, calculated according to the expression LOD = 3*s*/*a*, where "*a*" is the angular coefficient of the curve MM_{20} and "*s*" is the standard deviation of 10 measurements of an analytical blank. The LOQ of 30.0 µg/L for all evaluated elements was estimated as the lower linearity limit of the respective calibration curves. The mouthwash used in the migration test was previously diluted fivefold in 2.0% HNO_3 solution, and the analytical signals obtained for chromium, iron, and nickel were comparable to the blank (2.0% HNO_3). The results shown in Figure 1 cannot be used to affirm any contamination of the mouthwash by these metals. As a result, a more rigorous migration test would be necessary.

Zinc Quantification in Commercial Samples

Four mouthwash samples containing zinc salts in their formulations were purchased in the local market, and zinc quantification was performed using external calibration. 40 µL of each sample was diluted in 10 mL of 2.0% HNO_3 solution and analyzed by ICP-OES (n = 3). Results are shown in Table IV.

Detection and quantification limits for zinc were 5.0 µg/L and 30 µg/L, respectively, also calculated as described in the previous section "Quantification of Metal Migration from Stainless Steel," using the angular coefficient of the external calibration.

The amount of Zn^{2+} or zinc salts is not declared in most of the product labels, so it is not possible to make a comparison. The European Council (Regulation EC 1223/2009) sets 1.0% (by mass) as the maximum zinc content allowed in cosmetic products.

Conclusion

Statistical evaluation of the angular coefficients of calibration curves based on the Student's *t*-test allowed us to evaluate the matrix effects in the elemental analysis of mouthwash and guided the strategies to minimize these effects. The simple 250-fold dilution of the mouthwash samples was sufficient for zinc determination in commercial samples using external calibration, and matrix-matched calibration made it possible to quantify chromium, iron, and nickel at low concentrations while eliminating the matrix effect, simply and quickly, highlighting the small dilution factor. Excellent recovery percentages, low LODs and LOQs, and a wide calibration range for all evaluated elements show that simple strategies can be employed for elemental analysis in complex matrices, using ICP-OES.

Acknowledgments

The authors are grateful to the Multiuser Central Facilities (UFABC) for experimental support.

References

(1) P. Boyle, A. Koechlin, and P. Autier, *Oral Dis.* **20**(Suppl. I), 1–68 (2014).

(2) A. Young, G. Jonski, and G. Rölla, *Int. Dent. J.* **53,** 237–242 (2003).

(3) E.G. Winkel, S. Roldan, A.J. Winkelhoff, D. Herrera, and M. Sanz, *J. Clin. Periodontol.* **30,** 300–306 (2003).

(4) S. Saad, J. Greenman, and H. Shaw, *Oral Dis.* **17,** 180–186 (2011).
(5) J.R. Cortelli, M.D.S. Barbosa, and M.A. Westphal, *Braz. Oral Res.* **22**(Spec. Iss. 1), 44–54 (2008).
(6) H. Kerosuo, G. Moe, and E. Kleve, *Angle Orthod.* **65,** 111–116 (1995).
(7) G.S. Dolci, L.M. Menezes, R.M. Souza, and B.A. Dedavid, *R. Dental Press. Ortodon. Ortop. Facial.* **13,** 77–84 (2008).
(8) A.T. Erdogan, D. Nalbangtil, F. Ulkur, and F. Sahin, *Angle Orthod.* **85,** 665–672 (2015).
(9) W.B. Jones, G.L. Donati, C.P. Calloway Jr., and B.T. Jones, *Anal. Chem.* **87,** 2321–2327 (2015).
(10) G. A. Zachariadis, and E. Sahanidou, *Cent. Eur. J. Chem.* **9,** 213–217 (2011).
(11) F. C. Pinheiro, A.I. Barros, and J.A.A Nóbrega, *Anal. Chim Acta* **1065,** 1–11 (2019).
(12) J.L. Todolí, L. Gras, V. Hernandis, and J. Mora, *J. Anal. At. Spectrom.* **17,** 142–169 (2002).
(13) J. Porcayo-Calderon, M. Casales-Diaz, V.M. Salinas-Bravo, and L. Martinez-Gomez, *Bioinorg. Chem. Appl. 2015*, 1–14 (2015).
(14) D. Nalbantgil, F.Ulkur, G. Kardas, and M. Culha, *Bio-Med. Mater. Eng.* **27,** 539–549 (2016).

P. M. F. Camargo Filho, J. F. S. Joca, and I. Gaubeur are with the Molecular and Atomic Spectroscopy Laboratory at the Universidade Federal do ABC (UFABC), in Santo André, Brazil. Direct correspondence to: ivanise.gaubeur@ufabc.edu.br

Continued from page 27

(4) F. Vanhaecke, L. Balcaen, I. Deconinck, I. De Schrijver, C. Marisa Almeida, and L. Moens, *J. Anal. At. Spectrom.* **18**, 1060–1065 (2003).
(5) S.D. Fernandez, N Sugishama, J.R. Encinar, and A. Sanz-Medel, *Anal. Chem.* **84**, 5851–5857 (2012).
(6) N. Sugiyama, "The accurate measurement of selenium in twelve diverse reference materials using on-line isotope dilution with the 8800 Triple Quadrupole ICP-MS in MS/MS mode" (Agilent publication 5991-0259EN, 2012).
(7) Handbook of ICP-QQQ Applications using the Agilent 8800 and 8900, (Agilent publication 5991-2802EN, 2019).
(8) V.G. Anicich, *Astrophys. J., Suppl. Ser.* **84**, 215–315 (1993).
(9) V.V. Lavrov, V. Blagojevic, G.K. Koyanagi, G. Orlova, and D. K. Bohme, *J. Phys. Chem. A*. **108**, 26, 5610–5624 (2004).
(10) N. Sugiyama and K. Nakano, "Reaction data for 70 elements using O_2, NH_3 and H_2 gases with the Agilent 8800 Triple Quadrupole ICP-MS" (Agilent publication 5991-4585EN, 2014).
(11) L. Balcaen, E. Bolea-Fernandez, M. Resano, and F. Vanhaecke, *Anal. Chim. Acta* **809**, 1–8 (2014).

Ed McCurdy and Glenn Woods are with Agilent Technologies in Stockport, United Kingdom. **Naoki Sugiyama** is with Agilent Technologies International, in Tokyo, Japan. Direct correspondence to: ed_mccurdy@agilent.com

For more information on this topic, please visit our homepage at: www.spectroscopyonline.com

Spectroscopy

Solutions for Materials Analysis

Follow us on social media

Join your colleagues in conversation and stay up-to-date on breaking news, research, and trends associated with the spectroscopy industry.

"Like" and follow us on Facebook, LinkedIn, and Twitter today!

SpectroscopyOnline.com

MARS™ 6

Microwave Digestion System

The leader in microwave digestion

Better digestions. Better analyses.

iPrep™

The world's most robust vessel

iWave™

Accurate, contactless temperature control

iLink®

Remote system operation

One Touch™

It's like having a chemist in a box

CEM We Simplify Science

cem.com/MARS6